



Metal slanted columnar thin film THz optical sensors

Journal:	2011 MRS Fall Meeting
Manuscript ID:	Draft
Manuscript Type:	Symposium CC
Date Submitted by the Author:	n/a
Complete List of Authors:	Hofmann, Tino; University of Nebraska-Lincoln Schmidt, Daniel; University of Nebraska-Lincoln Boosalis, Alexander; University of Nebraska Lincoln, Electrical Engineering Kuehne, Philipp; University of Nebraska Lincoln, Electrical Engineering Herzinger, Craig; J.A. Woollam Co. Woollam, John; J.A. Woollam Co. Schubert, Eva; University of Nebraska Lincoln, Electrical Engineering Schubert, Mathias; University of Nebraska-Lincoln, Electrical Engineering
Keywords:	nanostructure, optical properties, dielectric properties

Metal slanted columnar thin film THz optical sensors

T. Hofmann¹, D. Schmidt¹, A. Boosalis¹, P. Kühne¹, C.M. Herzinger², J.A. Woollam², E. Schubert¹, and M. Schubert¹

¹University of Nebraska-Lincoln, Lincoln, NE, USA.

²J.A. Woollam Co., Lincoln, NE, USA.

ABSTRACT

We demonstrate that the anisotropic optical response of metal (cobalt) slanted columnar thin films (STF) at THz frequencies strongly depends on the dielectric properties of the dielectric ambient surrounding the slanted columnar thin films. An effective medium dielectric function approach is used to describe the combined optical response of metal slanted columnar thin film and dielectric ambient. Our observations indicate that metal (cobalt) slanted columnar thin films can be used as sensors which will enable detection and characterization of minute amounts of dielectrics at THz frequencies, such as for flow-based detection of liquid chemical constituents.

INTRODUCTION

Metal sculptured thin films (STFs) present an interesting class of self-organized, artificially made materials with three-dimensional, highly spatially coherent arrangements of nanostructures. The optical properties of STFs can differ significantly from the constituent material's bulk form [1, 2]. The physical properties of the STFs can be changed by varying the material, geometry, and scale of the nanostructures. We have shown recently that STFs prepared from electrically conductive materials offer the interesting opportunity to design transparent materials with very large dielectric polarizabilities [3,4,5,6]. The microscopic origin of the large dielectric polarizability of the STF is the high spatial coherence of electrically insulated arrays of sub-wavelength dipole antennas. The coupling between adjacent dipoles results in an electromagnetic response, which is strongly directional dependent and can be observed as optical anisotropy. Although some information is available on the anisotropic optical properties of metal STFs, very little is known on the effect of the dielectric properties of the ambient medium on the optical response of metal STFs.

In this work, we demonstrate that the anisotropic optical response at terahertz (THz) frequencies strongly depends on the dielectric properties of the ambient surrounding the slanted columnar thin films. Exemplarily we show the difference in the THz range response between STFs in air and STFs immersed in water here. Generalized spectroscopic ellipsometry (GSE) in the THz spectral range, which has become available very recently is employed here as a tool for the determination of the anisotropic dielectric properties of STFs [7,8,9,10]. We show furthermore that from accurate measurement of the anisotropic response of the STFs the dielectric properties of the medium surrounding the nanostructures can be determined. This is of interest since THz electronic and optoelectronic devices will require accurate knowledge of the dielectric properties of all constituents in the THz frequency region in particular for dielectric materials which may not be available in bulk form to facilitate direct measurement. We demonstrate that the anisotropic Bruggeman effective medium theory (AB-EMA) can be used in order to accurately describe the anisotropic optical response of the STFs. Complementary angle-

resolved GSE measurements in the spectral range from 400 to 1680 nm and scanning electron microscopy (SEM) were performed in order to determine the thickness and structural parameters of the STF for comparison.

THEORY

The anisotropic dielectric functions of Co STFs can be described by an anisotropic Bruggeman effective medium approximation (AB-EMA) [6]. In this approach, the Bruggeman formalism, which describes the homogenization for randomly oriented ellipsoidal inclusions is generalized for the case of highly oriented elliptically elongated inclusions [11]. The effective dielectric function tensor of the STF is described by the three major components ε_a , ε_b , and ε_c along the major axes a , b , and c of an orthorhombic system.

$$\varepsilon_j = \varepsilon_m + \frac{f(\varepsilon_i - \varepsilon_m)\varepsilon_j}{\varepsilon_j + L_j(\varepsilon_i - \varepsilon_j)},$$

where the dielectric permittivity and volume fraction of the nanocolumnar inclusions are denoted by ε_i and f , respectively. ε_m is the permittivity of the host medium, i.e., $\varepsilon_m=1$ for air, or $\varepsilon_m=\varepsilon_{\text{water}}$ for water, for example. L_j are the depolarization factors of the inclusions along their major polarizability axes. Regardless of inclusion shape, the sum of the three depolarization factors satisfies $L_a+L_b+L_c=1$. The dielectric permittivity of the metal nanocolumnar inclusions, ε_i , is described by the classical Drude formalism. A two term Debye formula was used to describe the dielectric permittivity of water $\varepsilon_{\text{water}}$ [12].

Stratified optical layer model calculations are needed to analyzed experimental THz-GSE data sets [13]. Here a four layer stratified layer model calculation composed of air ambient / Si substrate / Co STF / liquid cell medium was used. During the analysis the model calculated data were matched simultaneously as closely as possible to the experimental THz-GSE data sets by varying relevant physical model parameters (best-model).

EXPERIMENT

The sample studied in this work is composed of a 450 nm thick Co STF grown by electron-beam glancing angle deposition in a customized ultrahigh vacuum chamber. A double-side polished low phosphorous-doped n -type (001) silicon crystal was used as a substrate. The angle between the incident particle flux direction and the substrate normal was 85° during the sample growth. The slanting angle of the Co nanocolumns measured with respect to the substrate normal is 65° . A high-resolution field-emission SEM edge view image of the sample is shown in Figure 1 a). Details about the growth process are given in Ref. 3 and are omitted here for brevity.

A custom-built frequency-domain THz ellipsometers was used for the THz-GSE measurements presented here [9]. The THz-GSE data are represented using the Mueller matrix formalism [14]. The instrument is operating in polarizer-sample-rotating analyzer configuration, which allows access to the upper 3×3 part of the Mueller matrix [14]. Further information on the design of the instrument were reported in Refs. 7 and 9. During the measurements the sample was mounted onto a custom-build liquid cell with the Co STF facing the inside of the cell as shown in Fig. 1 b). Two measurements were carried out in the spectral range from 0.65 to 1.00 THz with a resolution of 1 GHz:

- i) with the empty cell (air ambient) and
- ii) with the cell filled with nanopure water.

The in-plane orientation of the sample was 225° during these experiments, i.e., the columnar slanting plane was oriented oblique to the plane of incidence in order to maximize the anisotropic optical response [6]. The angle of incidence was $\Phi_a=55^\circ$.

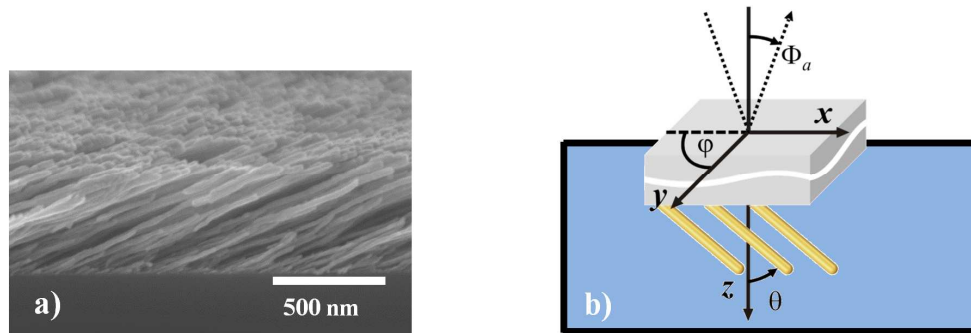


Figure 1. a) SEM micrograph of the investigated STF which is composed of slanted Co nanocolumns deposited by glancing angle deposition onto a silicon substrate. The slanting angle is 65° . Note that SEM micrograph was obtained with the sample tilted by 15° . b) Schematic of the experimental setup. The THz beam is reflected off the backside of the double-side polished low phosphorous-doped *n*-type (001) Si substrate. The Co STF is facing the inside of a custom-built cell, for which the liquid ambient can be exchanged.

RESULTS AND DISCUSSION

Figure 2 a) and b) depict the Mueller matrix spectra M_{12} , M_{21} and M_{33} of the Co STF sample at an angle of incidence of $\Phi_a=55^\circ$, respectively. The in-plane rotation was $\varphi = 225^\circ$. For comparison, the Mueller matrix spectra of the Co STF in air (empty cell) and immersed in the water are shown. The experimental (dotted lines) and best-model calculated (solid lines) data are

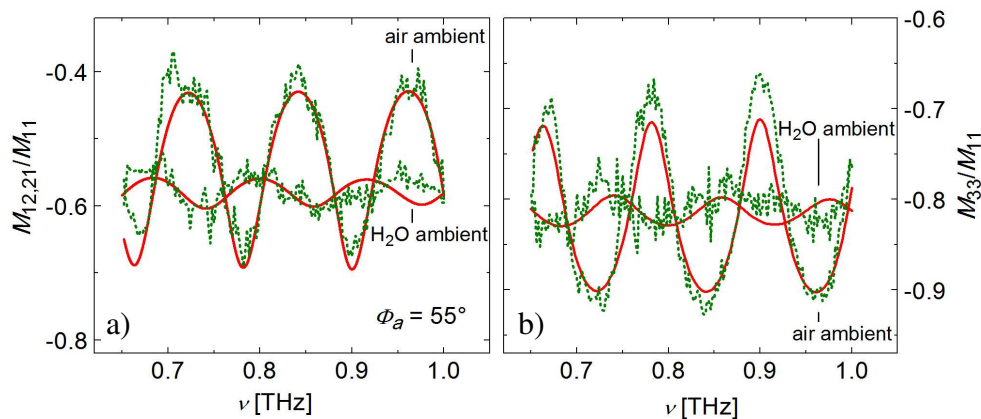


Figure 2. a) Experimental (dotted lines) and best-model calculated (solid lines) Mueller matrix spectra M_{12} and M_{21} obtained for the STF in air and immersed in water in comparison. b) shows the Mueller matrix spectra M_{33} .

found to be in very good agreement. The Mueller matrix spectra shown in Fig. 2 are dominated by a Fabry-Perot interference pattern, which originates from the double-side polished silicon substrate. The period of this interference pattern is determined by the layer thicknesses of all

sample constituents, but the major contribution is originating from the substrate which is (378 ± 1) μm thick. One can observe that the amplitude of the interference oscillation in M_{12} , M_{21} and M_{33} is reduced for the Co STF immersed in water compared to the Co STF in air ambient. The non-zero Mueller matrix spectra M_{13} , M_{31} , M_{23} , and M_{32} (Fig. 3) are evidence for the anisotropy of the optical response of the STF. The experimental and model calculated data are in very good agreement for both the STF in air and in water ambient. Similar to the isotropic Mueller matrix elements in Fig. 2 one can observe a decrease of the amplitude of the Fabry-Perot oscillations if the ambient of the STF is changed from air to water.

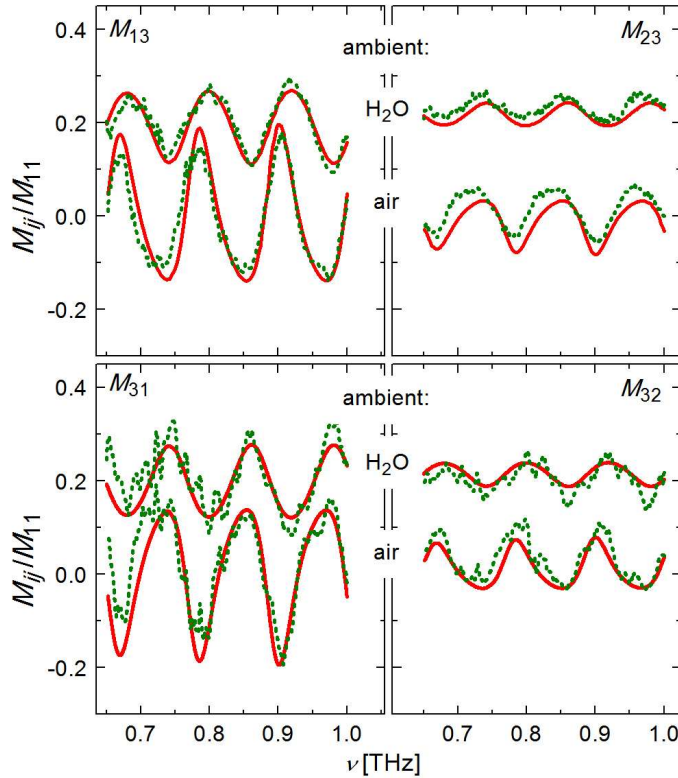


Figure 3. Experimental (dotted lines) and best-model calculated (solid lines) Mueller matrix spectra M_{13} , M_{31} , M_{23} , and M_{32} obtained for the STF in air and immersed in water.

The following best-model parameters were obtained for the STF thickness and volume fraction of the nanocolumns: $d=(441\pm 5)$ nm and $f=(33\pm 1)$, respectively. These parameters are in good agreement with SEM data obtained from Figure 1 a). The best-model parameters for the free charge carrier concentration and mobility of the silicon substrate are $N=(1.08\pm 4)\times 10^{15}$ cm^{-3} and $\mu=(1375\pm 111)$ $\text{cm}^2/(\text{Vs})$, respectively, assuming an electron effective mass of $0.26 m_0$ [15]. The slanting angle of the intrinsic Cartesian coordinate system of the polarizabilities ε_a , ε_b , and ε_c was found to be identical to the physical slanting angle of the nanocolumns. The following best-model parameters have been obtained for the AB-EMA depolarization factors: $L_a=0.3333\pm 10^{-4}$, $L_b=0.3355\pm 10^{-4}$, and $L_c=0.3313\pm 10^{-4}$ [6]. The best-model Drude parameters resistivity and scattering time for the Co nanostructures were $\rho=(1.2\pm 3)\times 10^{-5}$ Ωcm and $\tau=(239\pm 7)$ fs,

respectively. These parameters are in very good agreement with those obtained for a bulk-like 100 nm thick Co film deposited on a low doped silicon substrate for comparison.

If immersed in water the dielectric response of the Co nanostructures is screened. This can be clearly observed in a change of the AB-EMA depolarization factors: $L_a=0.3375\pm 10^{-4}$, $L_b=0.3373\pm 10^{-4}$, and $L_c=0.3252\pm 10^{-4}$. We furthermore observe changes in the best-model Drude parameters resistivity and scattering time for the Co nanostructures. The resistivity increases to $\rho=(1.1\pm 5)\times 10^{-4}$ Ωcm and the scattering time decreases to $\tau=(239\pm 10)$ fs. This might be attributed to continued oxidation of the Co nanocolumns. The best-model parameters obtained for the dielectric contribution of water are $\varepsilon_\infty=3.3\pm 5$, $\varepsilon_1=71\pm 4$, $\varepsilon_2=5.0\pm 1$, $\tau_1=8.3\pm 2$ ps, $\tau_2=0.18$ ps (not varied during analysis) which are in very good agreement with literature values [12].

CONCLUSIONS

In summary, we have demonstrated that the anisotropic optical response of Co STFs at THz frequencies strongly depends on the dielectric properties of the ambient surrounding the nanostructures. We have successfully employed an anisotropic effective medium dielectric function approach to describe the combined optical response of metal slanted columnar thin film and ambient. We find that the dielectric response of the Co nanostructures is screened by the ambient. These observations indicate that metal (cobalt) slanted columnar thin films can be used as sensors which will enable detection and characterization of minute amounts of liquids at THz frequencies. The AB-EMA model approach predicts upon slight modifications of Drude, fraction and/or depolarization parameters that targeted optical properties of STF in the THz range can be achieved by variation of slanting angle, lateral column density, and material.

ACKNOWLEDGMENTS

The authors would like to acknowledge financial support from the Army Research Office (W911NF-09-C-0097), the National Science Foundation (MRSEC DMR-0820521, MRI DMR-0922937, DMR-0907475, ECCS-0846329, EPS-1004094), the University of Nebraska-Lincoln, the J.A. Woollam Foundation.

REFERENCES

1. I.J. Hodgkinson and Q.H. Wu, *Birefringent Thin Films and Polarizing Elements* (World Scientific, Singapore, 1998).
2. M. M. Hawkeye and M. J. Brett, *J. Vac. Sci. Technol. A* **25**, 1317 (2007).
3. D. Schmidt, A. C. Kjerstad, T. Hofmann, R. Skomski, E. Schubert, and M. Schubert, *J. Appl. Phys.* **105**, 113508 (2009).
4. D. Schmidt, B. Booso, T. Hofmann, E. Schubert, A. Sarangan, and M. Schubert, *Appl. Phys. Lett.* **94**, 011914 (2009).
5. D. Schmidt, B. Booso, T. Hofmann, E. Schubert, A. Sarangan, and M. Schubert, *Opt. Lett.* **34**, 992 (2009).

6. T. Hofmann, D. Schmidt, A. Boosalis, P. Kühne, R. Skomski, C. M. Herzinger, J. A. Woollam, M. Schubert, and E. Schubert, *Appl. Phys. Lett.* **99**, 081903 (2011).
7. T. Hofmann, C. Herzinger, A. Boosalis, T. Tiwald, J. Woollam, and M. Schubert, *Rev. Sci. Instrum.* **81**, 023101 (2010).
8. T. Hofmann, A. Boosalis, P. Kühne, C. M. Herzinger, J. A. Woollam, D. K. Gaskill, J. L. Tedesco, and M. Schubert, *Appl. Phys. Lett.* **98**, 041906 (2011).
9. T. Hofmann, C. M. Herzinger, J. L. Tedesco, D. K. Gaskill, J. A. Woollam, and M. Schubert, *Thin Solid Films* **519**, 2593 (2011).
10. S. Schöche, J. Shi, A. Boosalis, P. Kühne, C. M. Herzinger, J. A. Woollam, W. J. Schaff, L. F. Eastman, M. Schubert, and T. Hofmann, *Appl. Phys. Lett.* **98**, 092103 (2011).
11. A. Sihvola, *Electromagnetic mixing formulas and applications* (The Institution of Electrical Engineers, London, 1999).
12. J. T. Kindt and C. A. Schmuttenmaer, *J. Phys. Chem.* **100**, 10373 (1996).
13. G. E. Jellison, *Thin Solid Films* **313-314**, 33 (1998).
14. H. Fujiwara, *Spectroscopic Ellipsometry* (John Wiley & Sons, New York, 2007).
15. M. van Exter and D. Grischkowsky, *Appl. Phys. Lett.* **56**, 1694 (1990).